JOURNAL OF MATERIALS SCIENCE **38** (2003) 3219 – 3222

Micro-beam plasma-arc surface processing for ferrous and nonferrous metals

M. YAN
National Key Lab of Silicon Materials, Zhejiang University, Hangzhou 310027, People's Republic of China
E-mail: mse_yanmi@dial.zju.edu.cn

In the paper a technique of surface treatment, micro-beam plasma-arc scanning, is reported. Surfaces of metals were melted by micro-beam plasma-arc and then self-quenched by the underlying substrates. The effects of surface treatment on the microstructure, wear and corrosion resistance of metals were investigated. The high self-quenching rates resulted in the refinement of microstructure, extended solubility of alloying elements, and even the formation of an amorphous structure. Wear and corrosion resistance of many alloys, particularly ferrous alloys, were improved. Reasons responsible for the effects are discussed.

1. Introduction

Wear, corrosion and fatigue are the most important phenomena responsible for failure of components. These failure mechanisms all occur at surfaces of materials, thus new technologies were developed to modify the surfaces. New technologies emerged while technologies considered to be traditional are improved or innovated. Surface treatment using low-power plasma-arc as the heating source to improve the corrosion or abrasion performance of components is developed from flame quenching and laser beam scanning, which is now investigated primarily in our laboratory [1–3].

Plasma-arc treatment uses a plasma arc to scan the component surface. A plasma arc, generated in a plasma gun, scans the surface, and this is followed by water spray quenching. In this case, the process is similar to flame quenching, although the temperature of plasma arc (over 50 000 K) is much higher than flame torch [4]. Using this process even amorphous structure formed at the surface of a plain carbon steel [5]. If the plasma arc is generated between the gun (which serves as the cathode) and the component surface (which serves as the anode), and the power input is not high (generally less than 200 W), the surface can be melted and self-quenched rapidly by the underlying substrate. In this case, the process is similar to laser beam surface scanning, although the energy density of plasma arc (10^5–10^6 W cm^{-2}) is lower than laser beam (10^5–10^9 W cm^{-2}) [6, 7]. This process is referred to as "micro-beam plasma-arc treatment" in our laboratory. Many metals, including plain carbon steels, alloy steels, gray irons, aluminum- and nickel-base alloys have been investigated through this treatment. This paper summarizes the main technological features of the micro-beam plasma-arc treatment, and some research results on materials.

2. Experimental

Primary experimental details have been described previously [1, 2], although some adjustment must be made for different alloys or for different objectives. A plasma arc was generated between plasma gun nozzle and the sample. The samples served as the anodes and the nozzle of plasma torch as the cathode. The plasma gun was controlled by a small variable speed DC motor; thus its speed could be adjusted throughout the test. This treatment can be carried in air, shielded by argon. Through multi-pass scanning, the whole surface of component can be treated. Pitches between adjacent passes were adjusted for different conditions, normally around 0.5 mm. The input power varied from tens to over one hundred watts. Technological objectives include avoiding bumps or holes at the treating surface, avoiding arc extinguishment, and obtaining scanning tracks as straight as possible.

The microstructures of samples were observed and analyzed through optical microscopy (OPM), scanning electron microscopy (SEM), transmission electron microscopy (TEM), and X-ray diffraction (XRD). Abrasion tests were conducted at room temperature with oil lubrication [1]. Corrosion resistance was determined through the measurement of polarization curves, or immersion tests [2]. The reference electrode was a saturated calomel electrode (SCE).

3. Results

During scanning the melt pool was not visible. The melting depths varied from tens to hundreds of microns, depending on the power input, the bulk material, and the scanning velocity. Scanning tracks of micro-beam plasma-arc on a plain carbon steel are shown in Fig. 1 [2]. Due to the minimum voltage principle of electric

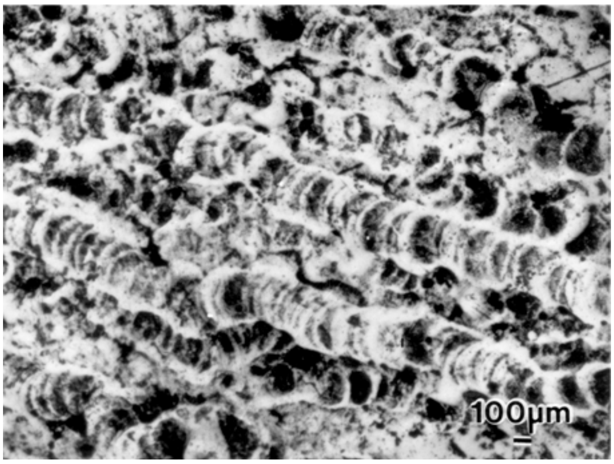

Figure 1 Scanning tracks on a carbon steel. Power input 81 W, scanning velocity 90 mm min^{-1}.

arcs, the plasma arc could drift off course, making the scanning track not very straight.

3.1. Ferrous alloys

In the investigated range of carbon from 0.15 to 0.65 wt%, the melting layers of plain carbon steels and low-alloy steels transformed to refined martensite. In the case of high carbon contents (over 0.3% C), small fractions of retained austenite could also be detected through XRD, due to the stabilizing effect of carbon on austenite. The martensite structure in the treated layer of a plain carbon steel containing 0.50 wt% carbon is demonstrated in Fig. 2.

For cast irons, in the melting layer no flake-shaped graphite could be found. The matrix comprised of refined ledburite, plus fine round-shaped graphite which distribute uniformly in the matrix. Since in cast irons the contents of carbon and silicon are high, graphite is prone to precipitate, and its nucleation can not be restrained completely. With the high self-quenching rates, precipitated graphite became refined round-shaped nodules. Microstructure of the melting layer in a cast iron containing 3.37% C, 2.08% Si and 0.83% Mn is demonstrated in Fig. 3.

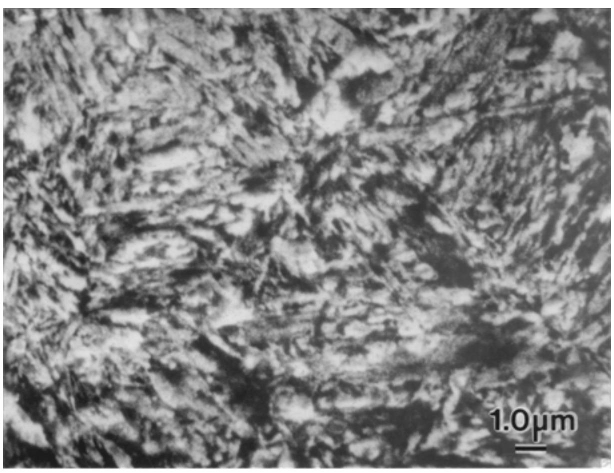

Figure 2 Surface microstructure of carbon steel after plasma-arc treatment. The steel contained 0.50% C. Power input 108 W, scanning velocity 90 mm min^{-1}.

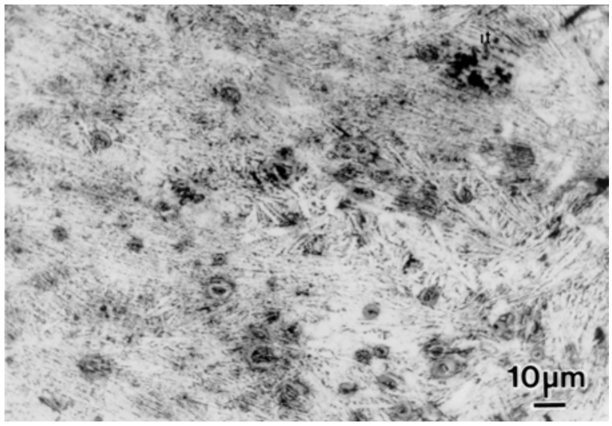

Figure 3 Surface microstructure of a cast iron after plasma-arc treatment. The chemical composition of iron was 3.37% C, 2.08% Si, 0.83% Mn, 0.12% P, 0.09% S, and Fe balance. Power input 135 W, scanning velocity 80 mm min^{-1}.

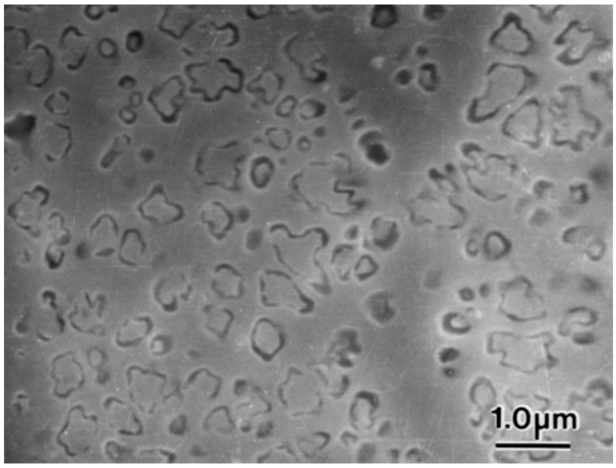

Figure 4 Refined precipitates in the plasma-arc treated layer of a ferrous alloy containing 4.2% C, 24.66% Cr, 3.1% Si and 2.4% B. Power input 54 W, scanning velocity 90 mm min^{-1}.

In the ferrous alloys containing high contents of alloying elements, in the melting layer carbides and other intermetallic compounds dissolved during plasma-arc heating. During subsequent cooling, compound particles could precipitate in refined forms, as displayed in Fig. 4 [1]. XRD indicated that owing to the solute entrapping effect of rapid solidification, a large amount of austenite could be retained at room temperature. Furthermore, through TEM observation it was found that amorphous structure could form in some areas at the top surface of high-alloying ferrous alloys [3].

For all ferrous alloys plasma-arc treatment improved the wear resistance significantly, particularly the abrasion resistance. This is because after treatment the surface hardness was increased greatly. For plain carbon steels or low-alloy steels, the increase of hardness was primarily due to forming of martensite. For high-alloy steels, the increase of hardness was also related to the increase of solubility of carbon in the matrix, as well as refinement of the structure.

The effect of plasma-arc treatment on the general electrochemical corrosion behavior heavily depended on the type and amount of alloying elements

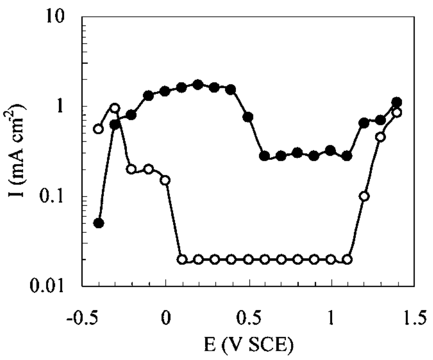

Figure 5 Anodic polarization curves of a low-alloying steel containing 5.0% Cr, 1.2% Mn, and 0.15% C in 1 N H_2SO_4. Power input 135 W, scanning velocity 80 mm min^{-1}, sweep rate 0.1 V per 5 minutes. **o**: treated surface, •: untreated surface.

in the material. Since plain carbon steels contain no alloying elements other than carbon in them, it was found that plasma-arc treatment couldn't improve their electrochemical corrosion resistance [8]. For alloy steels, due to the dissolution of carbides, such as (Cr, Fe)$_7$C$_3$, and the homogenization effect of rapid melting-solidification process, plasma-arc treatment drastically enhanced the passivation ability. Fig. 5 shows the anodic polarization curves of a low-alloying steel in 1 N H_2SO_4 solution. The steel contains 5.0% Cr, 1.2% Mn and 0.15% C. The passivation ability of the relatively low alloy steel was improved significantly after plasma-arc treatment. Important indexes like the critical current density for passivation, the current density in the passive regions, and the initial passivation potential were all lowered after treatment.

3.2. Non-ferrous alloys

The investigated nonferrous alloys included several aluminum alloys and nickel alloys. Since the crystal structure of aluminum or nickel does not change after solidification, so after plasma-arc treatment the most significant variation of these alloys in microstructure of surface layers was the refinement of structure, as well as the extension of solid solubility in the matrix. As a result, the surface hardness of aluminum and nickel alloys could be raised by plasma-arc treatment. For the A356 alloy (Al-7%Si–0.3%Mg), which is a typical and widely applied Al-Si alloy, the microhardness increased from HV 65 to HV 97 after 81 W plasma-arc scanning, and to HV 106 after 54 W plasma-arc scanning. Fig. 6 is an Al-12Si alloy. After plasma-arc treatment the structure of Al-Si eutectic in melting layer was greatly refined (the upper-left side of figure), the spacing of which was at the magnitude of hundreds of nanometers. The growth direction of laminar grains was from the substrate to the top surface.

However, the treatment could not significantly improve the corrosion resistance of aluminum alloys. The anodic polarization curves of an Al-alloy in 2 N H_2SO_4, with or without plasma-arc treatment, are given in Fig. 7. It can be seen that the critical current density for passivation and current density in the passive re-

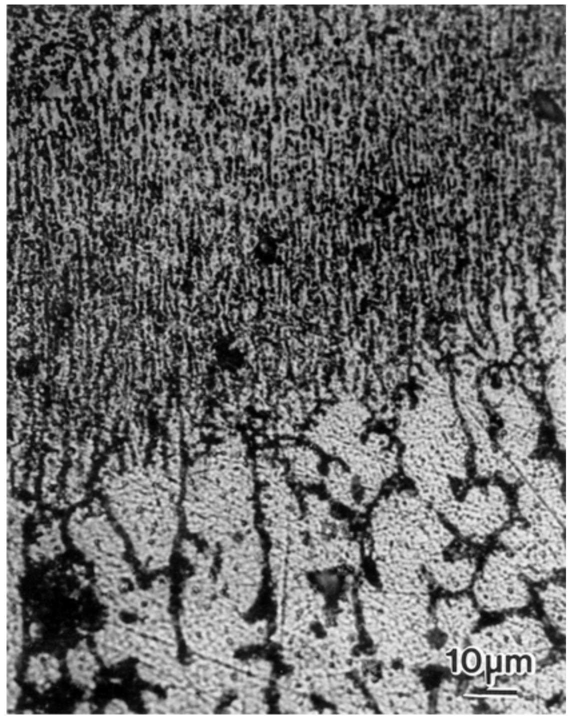

Figure 6 Refined laminar Al-Si eutectic in the melting layer of Al-12Si alloy. Power input 81 W, scanning velocity 36 mm min^{-1}.

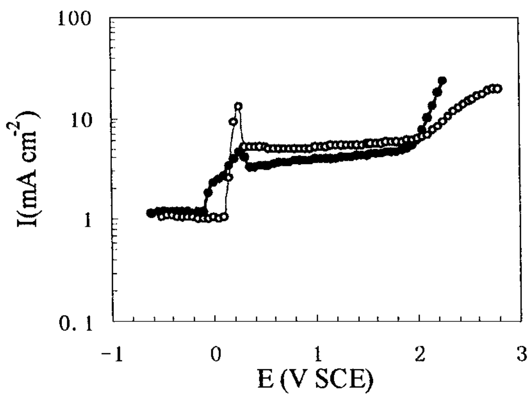

Figure 7 Anodic polarization curves of Al-alloy in 2 N H_2SO_4. The nominal composition of alloy was 0.30% Cu, 0.6% Si, 1.0% Mg, 0.2% Cr, Fe less than 0.7%, Al balance. Power input 81 W, scanning velocity 36 mm min^{-1}, sweep rate 0.1 V per 5 minutes. **o**: treated surface, •: untreated surface.

gion even increased a little after treatment. This may be attributed to the raised internal stresses in the surface layer.

Fig. 8 is a Ni-Cr-Si-B alloy (25.66% Cr, 3.41% Si, 2.82% B and 0.6% C) [2]. The melting layer was comprised of microcrystallites, 1–2 μm in diameter. After treatment, its microhardness was increased from HV 341 to HV 404 (54 W arc scanning), HV 419 (81 W arc scanning) and HV 423 (108 W arc scanning). The increase of hardness primarily resulted from the increased solubility of solute elements and refinement of structure. Plasma-arc scanning also improved the corrosion resistance of the alloy to some extent. After treatment the critical current densities for passivation were lowered, but the current densities in the passive region kept almost unchanged.

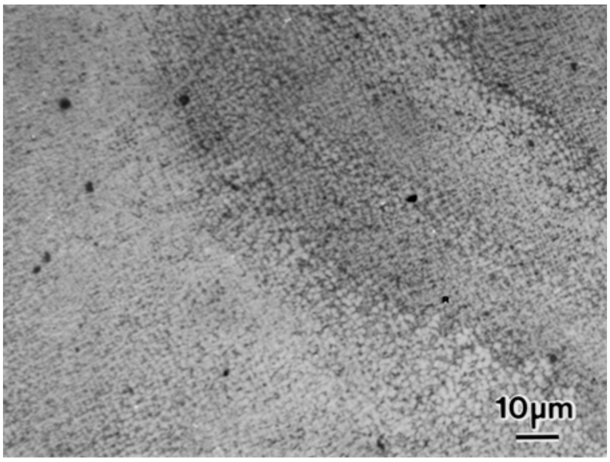

Figure 8 Microstructure of a nickel-base alloy containing 25.66% Cr, 3.41% Si, 2.82% B and 0.6% C after plasma arc treatment. Power input 54 W, scanning velocity 90 mm min^{-1}.

4. Discussion

Due to a flow of ionized gases heated to tens of thousands of degrees Celsius, the temperature of the plasma arc can be as high as 50000 K. Micro-beam plasma-arc treatment takes advantage of features of a plasma arc such as a high temperature and relatively high energy densities (10^5–10^6 W cm^{-2}) [4]. Since the arc focuses on a small point at the component surface, and thus heating is concentrated in a small area, the treatment subjects the surface layer of bulk material to a rapid solidification processing. Thus, plasma-arc scanning generally leads to refined surface microstructure, extended solubility of alloying elements, and homogenization of composition [9, 10]. This is why corrosion or abrasion resistance was improved.

Unlike the laser technique, the efficiency of surface heating with micro-beam plasma arc is not affected by the reflectivity of bulk surfaces; this is an advantage of plasma-arc scanning. However, good electrical conductivity of bulk materials is a prerequisite for the treatment. Surface cleanliness and roughness also affect the processing significantly. Thus it is necessary to clean or pretreat the surface before plasma-arc treatment. Iron- and nickel-base alloys have been confirmed to be suitable for processing, while aluminum alloys were found to be difficult to treat, since a dense Al_2O_3 film is present on the aluminum surface, and thus the arc is prone to extinguish during scanning. The technological features of the process are summarized in Table I, in comparison with those of flame quenching and laser beam surface treatment.

In view of the effect on wear and corrosion performance, as well as ease of processing for technological applications, micro-beam plasma-arc treatment is particularly suitable for various ferrous alloys.

TABLE I Main technological features of micro-beam plasma-arc treatment, flame quenching and laser beam surface treatment [2, 3, 6, 11–14]

	Plasma arc	Flame quenching	Laser beam
Density of energy	High	Low	Very high
Self-quenching rate	High	Low	High
Technical easiness	Excellent	Excellent	Good
Flexibility	Good	Excellent	Good
Equipment cost	Low	Low	High
Easiness for automatic operation	Good	Poor	Excellent

5. Conclusions

1. Micro-beam plasma-arc scanning has been proved to be an unique and promising approach, among various surface treatment processes. This process can achieve high self-quenching rates, resulting in variation and refinement of microstructure, extended solubility of alloying elements, and even the formation of amorphous structures.

2. Micro-beam plasma-arc treatment is particularly suitable to ferrous alloys, but not suitable to aluminum alloys due to technological difficulties. The process can significantly improve the wear resistance of various ferrous alloys, and improve the corrosion resistance of alloying steels/irons, and some nickel alloys.

References

1. M. YAN, *Surf. Coat. Tech.* **99** (1998) 132.
2. M. YAN and W. Z. ZHU, *ibid.* **92** (1997) 157.
3. *Idem.*, *Mater. Lett.* **34** (1998) 222.
4. H. Z. JIAN, "Welding Methods and Equipment" (Press of Mech. Industry, 1981) p. 97 (in Chinese).
5. H. C. LIN and R. G. DING, *J. Iron & Steel Res.* **5** (1993) 57 (in Chinese).
6. J. F. READ, "Lasers in Modern Industry" (Society of Manufacturing Engineer, Dearborn, Michigan, 1979).
7. P. A. MOLIAN, *Surf. Eng.* **1** (1986) 19.
8. M. YAN and W. Z. ZHU, *Surf. Coat. Tech.* **91** (1997) 183.
9. R. TRIVEDI, *Acta Met.* **34** (1986) 1663.
10. W. KURZ, *ibid.* **34** (1986) 823.
11. B. H. KEAR, E. M. BREINAN and L. E. GREENWALD, *Metals Tech.* **6** (1979) 121.
12. J. MEI and P. XIAO, in "Proc. of the 101st Annual Meeting & Exposition of the American Ceramic Society" (Indianapolis, 1999) p. 213.
13. C. W. DRAPER and J. M. POATE, *Inter. Metal Reviews* **30** (1985) 85.
14. W. M. STEEN, "Laser Cladding, Alloying and Melting" (Industrial Laser Handbook, 1986.)

Received 23 October 2002
and accepted 20 May 2003